

# Modeling And Simulation of a High Voltage Direct Current (HVDC) Bipolar Transmission Link for Long Distance Power Transfer

Godfrey Benjamin Zulu<sup>1</sup>, Conrad Chiswaka<sup>2</sup>, Charles Banda<sup>3</sup>

<sup>1, 2, 3</sup> Mulungushi University, School of Engineering, Department of Electrical and Electronics

## ABSTRACT

The increasing demand for electrical energy and the growing separation between generation sources and load centers have imposed significant challenges on conventional High Voltage Alternating Current (HVAC) transmission systems, particularly for long-distance bulk power transfer. High Voltage Direct Current (HVDC) transmission based on Voltage Source Converter (VSC) technology has emerged as a technically superior solution due to its controllability, reduced transmission losses and ability to connect weak or asynchronous power systems. Among Voltage Source Converter topologies, the Modular Multilevel Converter (MMC) has become the preferred configuration for high-voltage and high-power applications because of its modular structure, scalability and excellent harmonic performance. A comprehensive simulation-based study of a bipolar  $\pm 500$  kV MMC-VSC HVDC point-to-point transmission system designed for long-distance power transfer over approximately 800 km. Detailed mathematical models of the VSC, MMC arms, sub module capacitor dynamics, and DC transmission line are developed to describe the steady-state and dynamic behavior of the system. Control strategies for DC voltage regulation, active and reactive power control, circulating current suppression and capacitor voltage balancing are implemented and analyzed.

**Keywords:** Converter; Rectifier; Inverter; Thyristor-based converters; IGBT-based converters; PI controllers; Telegrapher's equations; DC-side dynamics; MATLAB/Simulink; ETAP; SOLIDWORKS; Asynchronous Interconnection; Weak AC grids; Distributed parameter line model; Point of Common Coupling; Network; Node; dq-frame; Thevenin Equivalent;

Date of Submission: 08-06-2026

Date of acceptance: 18-06-2026

## I. Introduction

The development of modern power systems has been accompanied by a growing need to transmit large quantities of electrical energy over long distances. In many countries, major generation sources such as hydroelectric power plants, large-scale renewable energy installations and thermal power stations are located far from major load centers. The increasing separation between generation and consumption has exposed fundamental limitations in conventional High Voltage Alternating Current (HVAC) transmission systems when applied to long-distance bulk power transfer [4][15][32].

HVAC transmission over long distances is constrained by reactive power flow, voltage instability, thermal limits and line charging effects. These limitations require the installation of multiple compensation devices and intermediate substations, which significantly increase system complexity and cost. As transmission distances approach several hundred kilometers, the technical feasibility and economic efficiency of HVAC systems deteriorate [1][2][4].

High Voltage Direct Current (HVDC) transmission provides an effective alternative for long-distance power transfer by eliminating reactive power flow along the transmission corridor and enabling precise control of power transfer. Recent advancements in power electronics have led to the widespread adoption of Voltage Source Converter (VSC) based HVDC systems. Unlike conventional transmission technologies, VSC-HVDC systems allow independent control of active and reactive power, support weak or passive AC networks and provide black-start capability. These features make VSC-HVDC particularly suitable for modern power systems

with in countries with weak grids such as Zambia’s very own with a  $SCR < 5$  and high penetration of renewable energy sources [1][6][7][12][15][32].

Among VSC topologies, the Modular Multilevel Converter (MMC) has emerged as the preferred solution for high-voltage applications due to its modular structure, scalability to very high voltage levels, low harmonic distortion and high efficiency. The MMC topology enables practical operation at voltage levels of  $\pm 500$  kV and above, making it suitable for long-distance bulk power transmission projects [9][10][11].

This research investigates a bipolar  $\pm 500$  kV MMC-based VSC-HVDC transmission system designed to transmit electrical power over a distance of approximately over 800 km. The fundamental problem addressed is whether such a system can operate stably and efficiently while maintaining effective control of DC voltage, active power, reactive power and internal converter dynamics. A simulation-based approach is adopted, consistent with industry practice and academic research standards [11][12][17][23][35][36].

This research is guided by the following key questions:

1. Which HVDC technology is optimal for Zambia’s long distance transmission needs?
2. Is simulation-based analysis sufficient to evaluate the performance such a large HVDC system/
3. How can converter stations and DC lines be mathematically modeled to capture steady-state and transient behavior?
4. What technical guidelines can support future HVDC planning in Zambia?

These questions are answered through detailed mathematical modeling and time-domain simulations of the proposed HVDC system. The simulation results demonstrate that stable DC voltage regulation is achieved, power transfer over the 800 km link is reliable and internal MMC dynamics are effectively controlled through appropriate control strategies. The results further confirm that simulation-based analysis provides a valid and reliable means of evaluating MMC–VSC–HVDC systems at this scale [16][25][26].

The major contribution of this paper is the development of a detailed simulation model, supported by theoretical analysis using the telegrapher’s equations, for a  $\pm 500$  bipolar MMC-VSC-HVDC transmission from large hydro generation in weak AC grids ( $SCR < 5$ ), representative of Zambia’s very own.

Thus, this research addresses a critical transmission problem faced by modern power systems and demonstrates that a bipolar  $\pm 500$  kV MMC-based VSC-HVDC transmission system is a technically viable and efficient solution for long-distance bulk power transfer. The findings of this study provide a strong technical foundation for the planning, design and analysis of future HVDC transmission projects [12][14][35].

A bipolar  $\pm 500$  kV voltage level was chosen for the HVDC link because this voltage provides an excellent balance between power transfer capacity (1500-2000MW), transmission efficiency over 850km and overall project demand. It also matches the generation capacity of Kariba Dam and represents a mature and proven technology level suitable for implementation in Zambia’s relatively weak grid environment.

## II. Methodology: System Architecture and HVDC System Mathematical Modeling

### 2.1 MMC-VSC-HVDC System Architecture

The proposed HVDC bipolar transmission system consists of five primary subsystems

1. AC System (Sending and Receiving ends)
2. Converter Station 1 (Rectifier)
3. HVDC Bipolar-Link
4. Converter Station 2 (Inverter)
5. Substations 1 (sending end) and 2 (receiving end)

These subsystems are interconnected through a  $\pm 500$  bipolar DC link from the sending end to the receiving end.

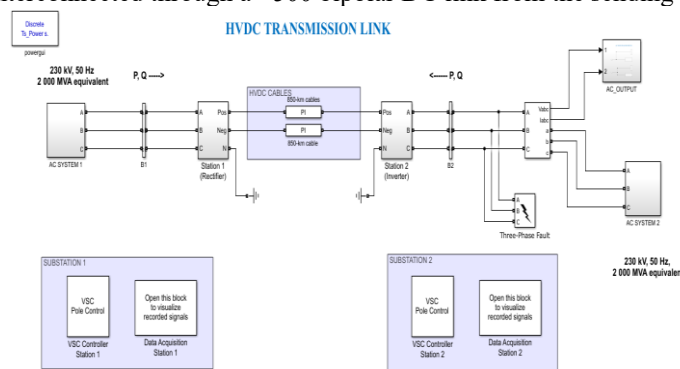


Figure 1: Overall Simulink HVDC model

AC System 1: The AC system 1 is the grid that delivers the stepped-up AC voltage to be seen by the converter transformer on the sending end of the whole system.

Converter Station 1: This is the converter that operates in rectifier mode to convert the incoming AC voltage into DC voltage to be transported over long distances by the bipolar link. This converter has a converter transformer preceding it that determines how much voltage can be injected into the rectifier to get the desired DC voltage in the link.

HVDC-Link: The bipolar cables whose potential is at both negative and positive. Because they are transporting DC voltage, they offer very less losses due to the fact that its reactance changes. Thus, they are very efficient over long distances. The PI controllers are employed to clear the steady state error and later re-stabilize the system after the error is cleared

Converter Station 2: The inverter is on the receiving end of the system. This inverter is the same converter as on the sending end and it operates in either rectifier or inverter mode, depending on the location. Thus, this receiving end converter converts the transported DC voltage with very fewer losses back into AC voltage to be fed into the receiving AC grid.

Substations 1 and 2: Substations 1 and 2 are data acquisition stations that are on both the sending and receiving ends of the transmission system. These stations control and monitor the subsystems that are connected to the converters. They record system performance data such as input and output voltage, current, disturbances, etc.

**System Parameters**

Parameter	Value
Grid voltage	230kV
Grid frequency	50Hz
Short circuit ratio (SCR)	≤3
DC-Link voltage	±500kV
DC-Link power	1500MW
DC-Link length	>800km
DC line resistance	0.05Ω/km
PWM switching frequency	200kHz
DC-Link capacitor	150uF
Proportional gain Pk	2,1
Integral gain Ki	189
Converter losses	1-2%

Table 1: Table showing employed parameters

**2.2 System Modelling**

A model is a mathematical representation of a system. In this paper, we shall limit ourselves to the converter transformer, converter stations 1 and 2, HVDC-Link and the substations.

**2.2.1 Converter Transformer Model**

The converter transformer before the rectifier is at the Point of Common Coupling. It performs electrical isolation for safety, steps up or down the AC grid voltage as per MMC requirement, performs filtering and an optional phase shift. In dq-reference frame, the equivalent circuit is modeled as shown:

$$v_{gd} = R_t i_d + L_t \left( \frac{di_d}{dt} \right) - \omega L_t i_q + v_d$$

$$v_{gq} = R_t i_q + L_t \left( \frac{di_q}{dt} \right) + \omega L_t i_d + v_q$$

Parameter	Description
R <sub>t</sub>	Transformer resistance
L <sub>t</sub>	Transformer leakage inductance
v <sub>d</sub> , v <sub>q</sub>	Converter side voltages
v <sub>gq</sub> , v <sub>gd</sub>	Grid side voltages at PCC

**2.2.2 Converter Station Model**

The converter is modeled from switching to average model

**Three-level:**

For a three-level converter, each phase leg switches between:

- $+\frac{V_{dc}}{2}$
- $-\frac{V_{dc}}{2}$

Using PWM, the average phase voltage over one switching period is

$$v_{conv, a} = ma \frac{V_{dc}}{2}$$

Here the d0 state of the average Vdc is lost because it is not a voltage source, it does not add any value to the energy and it only redistributes time. Nonetheless, the converter still remains a three-level.

**MMC:**

Unlike a three-level converter, the MMC does not have a fixed number of voltage levels. In real HVDC systems, we usually have over 200 submodules per arm.

$$\text{Number of Voltage levels} = 2N + 1$$

If N is, let's say 10 submodules per arm, then this means that we have 21 levels.

**Power balance:**

Just as the law of conservation of energy states, the converter does not create energy. It transfers energy between AC and DC domains.

The instantaneous power absorbed by the converter is:

$$P_{ac} = \frac{3}{2} (v_{did} + v_{qiq})$$

The DC power delivered to the DC system is:

$$P_{dc} = v_{dc} i_{conv}$$

If we neglect the losses, these two equations must be equal. By having this relationship, we can deduce the DC current drawn by the converter

$$i_{conv} = \frac{3 (v_{did} + v_{qiq})}{2 v_{dc}}$$

**2.2.3 HVDC-Link System Model**

The HVDC-Lines being large in length, are modeled using the distributed model as they are not a passive element but lines whose voltage and current values change with respect to time and distance/position on the line.

$$\begin{aligned} \frac{\partial v(x,t)}{\partial x} &= -ri(x,t) - l \frac{\partial i(x,t)}{\partial t} \\ \frac{\partial i(x,t)}{\partial x} &= -gv(x,t) - c \frac{\partial v(x,t)}{\partial t} \end{aligned}$$

Parameter	Description
r	Resistance per unit length Ω/km
l	Inductance per unit length H/km
g	Conductance per unit length S/km
c	Capacitance per unit length F/km

**DC-Link capacitor:**

Serves as an energy buffer between rectifier and inverter stations. Energy stored in the capacitor is

$$E_{dc} = \frac{1}{2} CV_{dc}^2$$

Differentiating wrt and applying power balance equation

$$CV_{dc} \frac{dV_{dc}}{dt} = P_{conv} - P_{dc}$$

where; Pconv is power from AC side and Pdc is power delivered to the DC transmission line

**Corona Effect:**

High voltage calls for a stronger field around a conductor. Air's breakdown field is less than or equal to 30kV/cm. When the conductor's field exceeds this threshold, air particles around that same conductor are ionized.

$$E_{max} = \frac{V}{r \ln \left( \frac{D}{r} \right)}$$

Thus, the corona starting point  $E_{max} \geq E_c$  (air’s breakdown strength, which is 30kV/cm).

**2.2.4 Substation System Model**

The substations comprise the controller and data acquisition systems. The dq-frame enables precise and decoupled control of the MMC and the Telegrapher’s equations ensure we account for the real long-distance line dynamics that can disturb this control.

**dq-Frame:**

d-axis current:  $L_g \frac{di_d}{dt} = v_{conv,d} - v_{g,d} - R_{gi}i_d + \omega L_g i_q$

q-axis current:  $L_g \frac{di_q}{dt} = v_{conv,q} - v_{g,q} - R_{gi}i_q - \omega L_g i_d$

where;

- $L_g \frac{di}{dt}$  is the energy stored in the AC receiving side inductance
- $v_{conv} - v_g$  is the potential difference between the inverter and grid
- $R_{gi}$  is the resistive power loss
- $\omega L_g i$  is the cross-coupling due to the rotating reference frame

**Acquired signals:**

The instantaneous three-phase signals are transformed into the dq-reference frame for analysis, where  $\theta = \omega t$  is the transformation angle obtained from the Phase-Locked Loop (PLL).

$$X(k) = \sum_{n=0}^{N-1} x(n)e^{-j2\pi kn/N}$$

This allows for quantification of Total Harmonic Distortion (THD):

$$THD = \sqrt{\sum_{h=2}^H \left(\frac{X_h}{X_1}\right)^2} \times 100\%$$

**III. Simulation Realization**

The MMC-VSC-HVDC system was realized on Simulink and ETAP.

**3.1 MATLAB/Simulink**

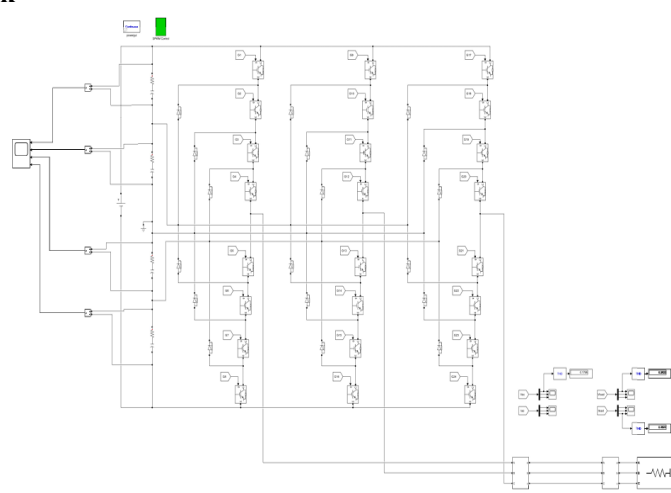


Figure: 2 MMC converter

The waveform of this simulation model shows the voltage with large visible steps. This is because this simulation model employs a small number of sub modules. Commercial MMC systems use over 200 sub modules per arm, which produce a much smoother waveform. Three-level has only three voltage levels, so in idealized plots it can sometimes look neater while still having much higher harmonics, a problem we intend to tackle with MMC. With this being stated, MMC offer very little filter requirements compared to three-level converters as shown in figure 3 below:

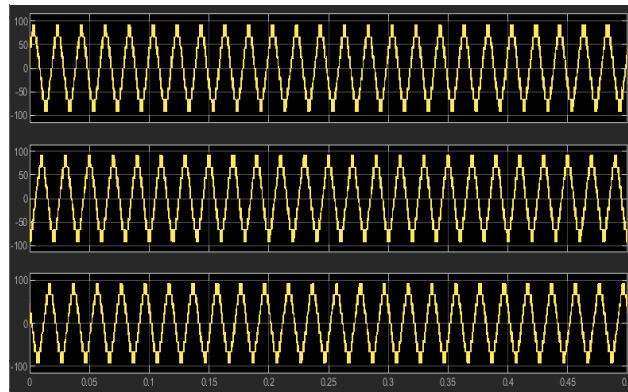


Figure 3: Waveform of an MMC

Figure 4 shows the waveform of a three-level Voltage Source Converter. Since the converter only has three voltage levels, the sinusoidal waveform is not close to being smooth, unlike the MMC. Thus, there is still more harmonic distortion and the system using such a converter will therefore need more filters.

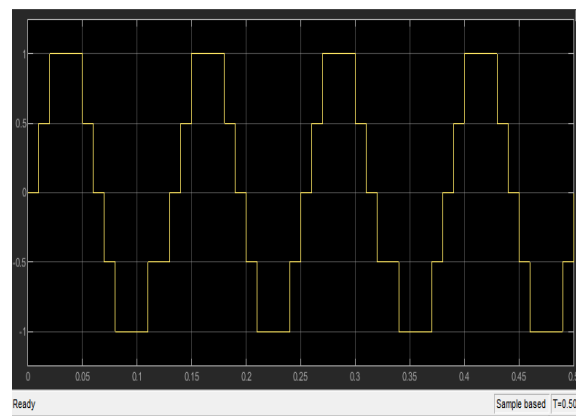


Figure 4: Waveform of a three-level

We can then safely say the superior waveform quality of the MMC is mainly attributed to its high number of voltage levels, which approximates a pure sine wave. Although the current simulation used moderate number of submodules, real-world systems with 200-400 submodules per arm achieve even smoother outputs. Better still, this result shows that MMC stands firm for high voltage, long distance transmission than traditional three-level converters, especially in terms of power quality, efficiency and filter requirements.

**VSC Discrete controller:** The controller processes measured voltages and currents from the AC and DC sides. This controller implements hierarchical control in the dq synchronous reference frame, with PI regulators for current, active power and DC voltage regulation, as shown below;

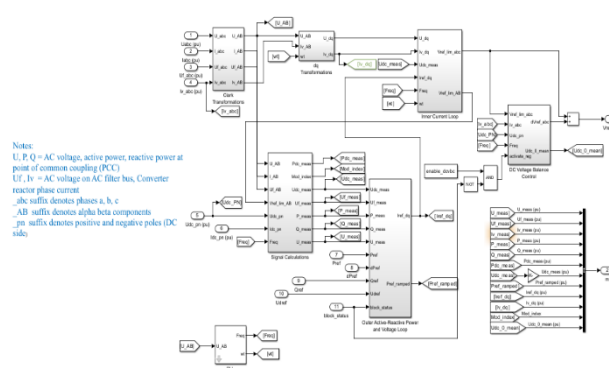


Figure 5: Discrete PI controller

**VSC Station:** The converter stations incorporate comprehensive control and data acquisition system. The system includes anti-aliasing filters, dq transformations, inner current control loops, outer power and voltage control loops and modulation signal generation.

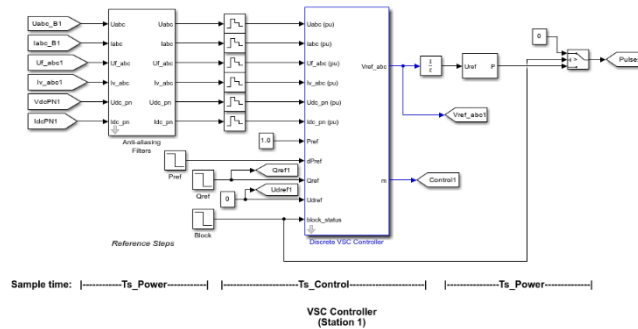


Figure 6: Internal of VSC station

**Data acquisition:** Presents detailed signal flow, including power calculations, reference generation and voltage balance control. Data acquisition is performed continuously to monitor key variables. These signals are essential for real-time control, performance evaluation and post-simulation harmonic analysis using FFT.

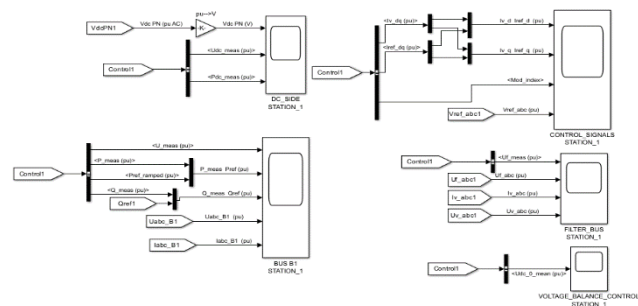


Figure 7: Internal of data acquisition block

**3.2 ETAP**

The figure below shows the setup of an HVDC transmission system on ETAP.

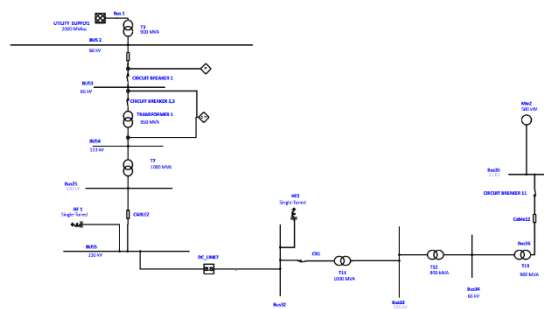


Figure 8: ETAP model of an HVDC link

**IV. Conclusion**

This research modeled a point-to-point  $\pm 500\text{kV}$  MMM-VSC-HVDC bipolar transmission system and converter stations using VSC technology. It investigated and compared the performance of two voltage source converters topologies with a focus on which offers less filter requirements as a result of less harmonics. Using a base power scaled to the national grid, Simulink models were developed. The outcomes clearly demonstrated that while three-level converters offer simpler control implementation and lower complexity, it produces significant harmonic content, necessitating large AC filters and losses. In contrast, MMC generate a near sinusoidal waveform provided the sub modules are more. Such a converter generates very low harmonic distortion even before filtering. This superior waveform quality significantly reduces filtering requirements, lowers transmission losses and improves power quality---merits that are particularly valuable for long distance

HVDC links. This research analyzed the DC bipolar cables using the telegrapher's equations because for long-distance HVDC the transmission line is not a simple resistor, it has distributed parameters that create traveling wave effects and dynamic interactions with the converter. Understanding this interaction at the sending end is essential for realistic stability and performance evaluation.

### References

- [1] J. Arrillaga, *High Voltage Direct Current Transmission*, 2nd ed., London, UK: IET, 1998.
- [2] K. R. Padiyar, *HVDC Power Transmission Systems*, New Delhi, India: Wiley Eastern, 1990.
- [3] N. Hingorani and L. Gyugyi, *Understanding FACTS*, New York, NY, USA: IEEE Press, 2000.
- [4] P. Kundur, *Power System Stability and Control*, New York, NY, USA: McGraw-Hill, 1994.
- [5] C. M. Franck, "HVDC transmission systems," *IEEE Trans. Power Del.*, vol. 28, no. 4, pp. 2141–2149, 2013.
- [6] E. Kimbark, *Direct Current Transmission*, New York, NY, USA: Wiley, 1971.
- [7] ABB, *HVDC Light® Technology Overview*, ABB Technical Report, 2018.
- [8] J. Reeve, "HVDC transmission," *IEEE Power Engineering Review*, vol. 8, no. 8, pp. 11–15, 1988.
- [9] R. Marquardt, "Modular multilevel converter," *Proc. IEEE*, vol. 98, no. 4, pp. 662–676, 2010.
- [10] S. Allebrod, R. Hamerski, and R. Marquardt, "New transformerless, scalable modular multilevel converters," *IEEE PES*, 2008.
- [11] L. Harnefors et al., "Control of MMC-based HVDC systems," *IEEE Trans. Power Syst.*, vol. 29, no. 2, pp. 703–712, 2014.
- [12] CIGRÉ WG B4.37, *VSC HVDC Systems*, Technical Brochure 604, 2014.
- [13] J. Yang et al., "DC fault protection of HVDC grids," *IEEE Trans. Power Del.*, vol. 33, no. 4, pp. 1841–1852, 2018.
- [14] IEEE PES, *HVDC and FACTS Handbook*, IEEE Press, 2016.
- [15] M. P. Bahrman and B. K. Johnson, "The ABCs of HVDC transmission technologies," *IEEE Power and Energy Magazine*, vol. 5, no. 2, pp. 32–44, 2007.
- [16] J. Arrillaga and Y. Liu, *High Voltage Direct Current Transmission*. IET, 2018.
- [17] N. Flourentzou et al., *IEEE Trans. Power Electron.*, 2009.
- [18] G. P. Adam et al., *IEEE Trans. Power Delivery*, 2014.
- [19] S. K. Chaudhary et al., *IEEE Trans. Ind. Electron.*, 2013.
- [20] M. Liserre et al., *IEEE Trans. Power Electron.*, 2006.
- [21] CIGRÉ TB 604, 2014.
- [22] Z. Xu et al., *IEEE Access*, 2019.
- [23] A. Yazdani and R. Iravani, Wiley-IEEE, 2010.
- [24] N. R. Chaudhuri et al., Wiley, 2014.
- [25] A. M. Gole et al., *IEEE Trans. Power Delivery*, 2019.
- [26] H. Saad et al., *IEEE Trans. Power Delivery*, 2014.
- [27] H. Wang and F. Blaabjerg, *IEEE Trans. Power Electron.*, 2018.
- [28] ZESCO Ltd., National Power System Status Report, 2023.
- [29] SAPP, Annual Report, 2022.
- [30] Power Transmission Over Long Distances. Milana Lima Dos Santos, IEEE, Geraldo Luiz Costa Nicola, Thales Sousa, 2014.
- [31] Yazdani et al., IEEE TPWRD 2008.
- [32] U.S. Department of Energy, High-Voltage Direct Current transmission: A Primer, Washington, DC, USA, 2018.
- [33] Australian Government, project development and annual progress report, Canberra, ACT, Australia, 2022.
- [34] Hydro-Quebec, The Quebec-new England Phase II HVDC Transmission Project, Montreal, QC, Canada, Tech. Rep., 2019.
- [35] European Network of Transmission System Operators for Electricity (ENTSO-E), High Voltage Direct Current Transmission Technology and Applications, Brussels, Belgium, 2020.
- [36] C. Lui, Z. Xu, and H. Rao - Application and Development of ultra-high-voltage HVDC transmission in China. *IEEE Power and Energy Magazine*, vol. 14, no.2, pp. 43-51, Mar.-Apr.2016.
- [36] Hingorani, N.G (1996). "High-voltage DC transmission: a power electronics powerhouse". *IEEE Spectrum*.33(4): 63-72.
- [37] Breaking News- The Chinese Government Website.
- [38] VSC Transmission, CIGRÉ Technical Brochure No. 269 Archived 2016-02-04 at the Wayback Machine, 2005.
- [39] Advances in HVDC Systems: Aspects and Principles.
- [40] REN21, "Renewables 2012 Global Status Report," 2012 [Online]. Available: [www.ren21.net](http://www.ren21.net)
- [41] Shen, L., Barnes, M., Milanovic, J.V. et al.: 'Potential interaction between VSC-HVDC and STATCOM'. 18th Power System Computation Conf. (PSCC), August 2014 (Google Scholar)
- [42] Sharifabadi, K., Harnefors, L., Nee, H.P. et al.: ' Design, control, and application of modular multilevel converters for HVDC transmission systems' (John Wiley & Sons, Inc., NJ, USA, 2016) (Google Scholar)
- [43] Davidson, C.: 'HVDC for securing supply'. Available at <http://www.offshorewind.biz>, accessed 30 May 2016 (Google Scholar)
- [44] Ahmed, N., Ångquist, L., Norrga, S. et al.: 'A computationally efficient continuous model for the modular multilevel converter', *IEEE J. Emerg. Sel. Top. Power Electron.*, 2014, 2, (4), pp. 1139–1148 (Google Scholar)
- [45] Cole, S., Beerten, J., Belmans, R.: 'Generalized dynamic VSC MTDC model for power system stability studies', *IEEE Trans. Power Syst.*, 2010, 25, (3), pp. 1655–1662 (Google Scholar)
- [46] Svensson, J.: ' Grid-connected voltage source converter control principles and wind energy applications'. PhD dissertation, School of Electrical and Computer Engineering, Chalmers University of Technology, 1998
- [47] Wang, W.: ' Operation, control, and stability analysis of multi-terminal VSC-HVDC systems'. PhD dissertation, School of Electrical and Electronic Engineering, The University of Manchester, 2015
- [48] Arunprasanth, S., Annakkage, U.D., Karawita, C. et al.: 'Generalized frequency-domain controller tuning procedure for VSC systems', *IEEE Trans. Power Deliv.*, 2015, 31, (2), pp. 732–742
- [49] Durrant, M., Werner, H., Abbott, K.: 'Synthesis of multi-objective controllers for a VSC-HVDC terminal using LMIs'. *IEEE Conf. Decision and Control*, 2004, pp. 4473–4478
- [50] Pradhan, J.K., Ghosh, A., Bhende, C.N.: 'Small-signal modelling and multivariable PI control design of VSC-HVDC transmission link', *Electr. Power Syst. Res.*, 2017, 144, pp. 115–126